International Journal for Multidisciplinary Research (IJFMR)
E-ISSN: 2582-2160 ● Website: www.ijfmr.com ● Email: editor@ijfmr.com

Dynamic Characterization of Diameter for Round Surfaces Using a Non-Contact Optical Measurement System

Aynur Didem Oktan Karayeğen[1], Hüseyin Kurtuldu[2]

[1,2]Department of Biomedical Engineering, Baskent University, Ankara, Turkey

Abstract

Ensuring uniformity in the final round product's diameter is essential to production line operations because it permits adherence to geometry specifications and fulfills client demands. Non-contact diameter measurement systems are essential for manufacturing cost savings as well as quality monitoring. However, because of their non-linear movement, lengthy manufactured specimens like rods might be difficult to measure the diameter of precisely. Typically, analysis systems rely on costly and intricate optical components, limiting accessibility to small businesses. This research aims to address this issue by presenting a low-cost and practical optical system for measuring the diameters of round samples in continuous lines. The aim here is to obtain instant feedback through dynamic measurement and to create a continuous control mechanism that will contribute to sustainability. Experimental results show that the proposed method exhibits a high level of precision, with a measurement accuracy of 0.25% of nominal diameter.

Keywords: Optical Measurement, Rod Diameter, Digital Image Processing, Dynamic Characterization

1. Introduction

Cold drawing is a common metal forming process that involves the use of physical force to stretch and manipulate metal into a rounded shape[1]. This process is widely used by companies to produce various finished products, such as steel bars, gears, spokes, and bolts, among others, resulting in millions of miles of metal drawn annually. The precise control of diameter during production is essential, as it not only ensures compliance with quality standards, but also minimizes material consumption. Cold-drawn products, in particular, are subject to stringent tolerances on their nominal diameters, with the ASTM A108 standard[2] specifying a tolerance of 51 micrometers for nominal diameters up to 38 mm. Given the requisite accuracy, measurements are typically performed after the completion of production. However, early detection of any deviations in production is vital to reduce scrap and rework. Nevertheless, measuring tolerances during the early stages of drawing presents a challenge, as long products do not move in a straight line and tend to oscillate about half the diameter of round products (see supplementary video).

Over the past few years, there has been an increasing demand for precision and accurate systems for measuring geometric parameters[3–6]. Many instruments rely on telecentric illumination and imaging to measure samples that cannot be precisely positioned. Although telecentric lenses offer ideal magnification that does not vary with the working distance between the object and the camera, they are

relatively expensive and have a limited field of view. Dvoinishnikov et al.[7] showed that telecentric lenses can measure diameters of cylindrical objects up to 10 mm with a measurement accuracy of 0.24 µm when the samples are viewed in the same position. However, Li. et al.[8] found that the magnification of a telecentric system can be impacted by manufacturing and assembly errors of the lens, resulting in an error of approximately 20 microns for every 10 mm the object is moved from the lens.

Various studies have employed different optical techniques for measuring sample diameter. For instance, Radil et al.[9] used a lensless imaging method to analyze the shadowgraph profiles of samples viewed directly by a camera sensor. The study showed that a 0.3 mm diameter sample can be measured with an accuracy of 3 µm when moved 15 mm away from the sensor. However, the maximum diameter that can be estimated with this technique is limited by the sensor size. Sun et al.[10] used a regular camera and lens to estimate shaft diameters between 20 and 27 mm with an averaged error of 5 µm. In this study, measurements were made by clamping the shafts in a fixed position. Demeyere et al.[11] employed a triangulation technique, whereby the laser line profile of spherical objects was used to determine the diameter with a general accuracy of roughly 1% of the nominal diameter.

In Chen et al.`s study[12], the sample under examination was secured by positioning it on a support bar, with the utilization of a telecentric lens. Within this setup, the standard deviation was determined to be 10 µm for a 6 mm sample. In a separate study [13], images were captured and analyzed using a single camera. Samples of varying diameters were securely mounted onto a supporting bar, with the subsequent images subjected to detailed analysis. The findings revealed that samples within the 30-40 mm range exhibited a standard deviation of 15 µm upon examination. Rakhmanov et al.[14] aimed to assess the precision of diameter measurements by capturing images of samples from various angles. It has been noted that the standard deviation varies with the object's angle, with a reported range of 12 µm. Nevertheless, in this system, the object's range of motion is restricted.

Here, we introduce a novel optical system designed for the precise measurement of the diameter of round objects exhibiting non-linear movement, irrespective of their spatial orientation. Our proposed system represents a significant advancement over existing approaches, as it overcomes the limitations of traditional methods that are inherently sensitive to the position of the object being measured. Through the integration of both hardware and software components, our optical system achieves a high degree of precision and reliability, offering a promising solution for a wide range of industrial and scientific applications.

2. Experimental Procedure

The present study describes the design of an optical system (Figure 1(a)) that has been integrated into a translational stage (Figure 1(b)) for measuring the diameters of round objects. The system comprises a high-power LED (5W, 5000K), a convex lens with a focal length of 25 mm, a mirror, a converging lens with a focal length of 35 mm, a 10X objective lens (0.25 numerical aperture), and an achromatic lens with a diameter of 50 mm and a focal length of 180 mm. The collimated beam of light illuminates the sample, and its shadowgraph profile (Figure 1(c)) is imaged on a thin screen that is positioned between the sample and a 5-megapixel USB camera with a 10-50 mm variable imaging lens. To prevent chromatic aberration, a green filter is utilized before the achromatic lens, and it is chosen to match the wavelength range to which the sensor is maximally responsive.

The light source employed in the system has sufficient power to illuminate a viewing area of approximately 28 mm x 21 mm when the camera exposure is set to 1ms. Stroboscope measurements

were made to determine the maximum speed of the object at which the camera could capture clear images within this field of view and with these exposure settings. The results showed that an object moving with a linear speed of 10 m/s can be displayed clearly with our camera in the system.

To demonstrate the feasibility of the proposed system, the study utilizes two certified steel rods with mean diameters of 6.00 and 20.00 mm and a 0.01 mm deviation in diameter along their lengths. The rods are placed on a translation stage, which facilitates raster scanning along the axis perpendicular (x) and parallel (y) to the imaging direction (Figure 1(b)).

In order to determine the diameter of the samples at different scanning positions, interpolation-based algorithms are utilized to detect the edges of the rods with subpixel resolution [15]. Subpixel resolution refers to the ability of an imaging system or detector to resolve or distinguish between features that are smaller than a single pixel [16–18]. By improving the system's ability to resolve smaller features, it can increase the accuracy of measurement, and it can also help to overcome the limitations of the system's spatial resolution, which is determined by the pixel size and the numerical aperture of the lens18. In the case of sub-pixel image processing, the Savitzky-Golay filter can be used to perform smoothing and noise reduction on images that have been digitally zoomed or scaled down. This is because when an image is scaled, the pixels are often shifted by a fraction of a pixel, leading to uneven sampling and aliasing artifacts [19,20]. It involves fitting a polynomial function to a window of adjacent data points and using this function to estimate the smoothed value at the center point of the window. In the study, the most efficient result was obtained when the filter degree was 17 and the polynomial degree was 3. After these preprocessing applications, the resultant pixel positions of both sides of the rods are recorded. While the average pixel position difference method is the quickest and simplest approach to diameter calculation, it is susceptible to errors in instances where the sample is not perfectly aligned. As such, we propose two alternative and precise methods for diameter measurement (Figure 2). The first is the distance-based approach (DBM), which determines the diameter through calculation of the distance between the closest pair of pixels on both sides, using the Euclidean distance [21]. The diameter value is obtained by averaging 1920 distances along the sample. The second method, the slope-based approach (SBM), entails using two separate linear fits applied to the pixel clusters on both edges, which are then used to generate two parallel lines. The diameter is subsequently derived from the distance between these parallel lines [22]. With a 2.60GHz processor computer, the DBM and SBM methods yield respective measurement times of 0.429 seconds and 0.407 seconds for a single image.

Figure 1: (a) Schematic Representation of The Optical Components. Converging Lenses, Namely L1 (With a Focal Length of 25mm) and L2 (With a Focal Length of 35mm), a Pinhole (PH), a Mirror (M), an Objective Lens (OBJ), a Filter (F) an Achromatic Lens (L4), and a Screen (S). (b) Integration of The Optical System into a Translational System. (c) Snapshot of a Rod Captured by The Camera.

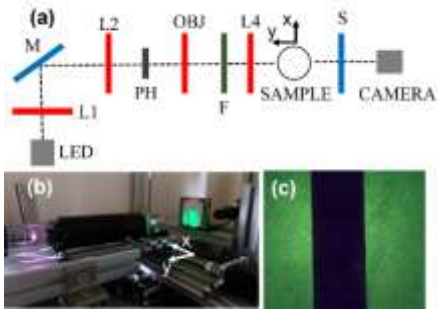

Prior to conducting experiments, the alignment of the optical components and camera is carried out by scanning the sample along the x and y directions to minimize diameter variations within the region between the achromatic lens and the screen. Once the system is optimized, the 6 mm and 20 mm diameter rods are scanned by the motorized stages with a resolution of 0.5 mm over areas of 20 mm x 40 mm and 8 mm x 40 mm, respectively. The pixel calibration is determined by measuring the diameter of the 6 mm rod in pixel units at the center position of the measurement region. The calculated pixel resolution of the system is 10.93 µm, which is subsequently used for calculating the actual diameters at different scan positions for both the 6 mm and 20 mm rods. Scanning the samples around the region center is employed to simulate oscillations on production lines (see supplementary video).

Figure 2: Edge Profiles Extracted from a Shadowgraph Image of the 6 mm Rod. The Dashed Line Depicts the Shortest Distance for The Closest Pair of Pixels. The Blue and Red Lines Represent the Linear Fits On Pixel Coordinates On Both Sides of The Rod ($y = m_1 + c_1$ and $y = m_2 + c_2$, Respectively). The Distance Between the Two Parallel Lines is Calculated from $|c_2 - c_1|/\sqrt{1 + m^2}$, Where m is The Average of m_1 and m_2.

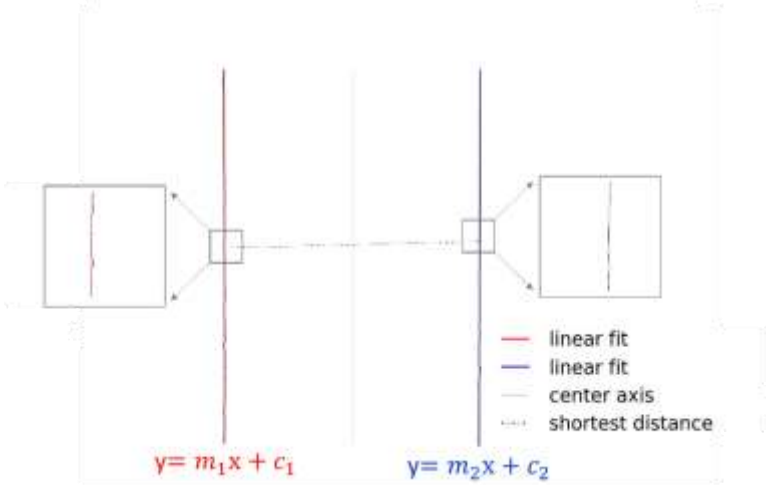

3. Results

The effects of sample orientation and measurement region length are investigated on the performance of DBM and SBM methods for the 6 mm nominal diameter rod. To assess these effects, different regions of interest (ROIs) are determined for the upright rod and the diameter of each ROI is measured. Specifically, a 100% ROI corresponds to the entire sample view, while a 50% ROI covers only the central half of the rod. Pixel calibration is obtained by measuring the diameter of the 6mm bar with 100% ROI in pixel units, and this factor is then used to calculate the diameter and deviation from the nominal diameter for other ROI values. The results, as shown in Figure 3(a), indicate that the DBM method is less sensitive to the number of edge pixels used in the calculations compared to the SBM method. Furthermore, both techniques provide an accuracy of approximately 3% of the nominal diameter when measured at the full length of the rod with sub-pixel resolution. Figure 3(b) illustrates the deviations for both methods when the rod is rotated by 3 degrees from its vertical position at the center of the measurement region. While a few degrees of rotation do not affect the measurements for both methods, the SBM method outperforms the DBM method as the rotation increases. This finding underscores the importance of proper alignment of the optical system. In real production settings, while

fluctuations about the center axis of the bars are expected, product rotation is unlikely as they are continuously produced in long lengths.

Figure 3: (a) Deviation in The Nominal Diameter of a 6 mm Rod as a Function Of (a) Region of Interest (ROI) and (b) Rotation Angle for The DBM and SBM Methods.

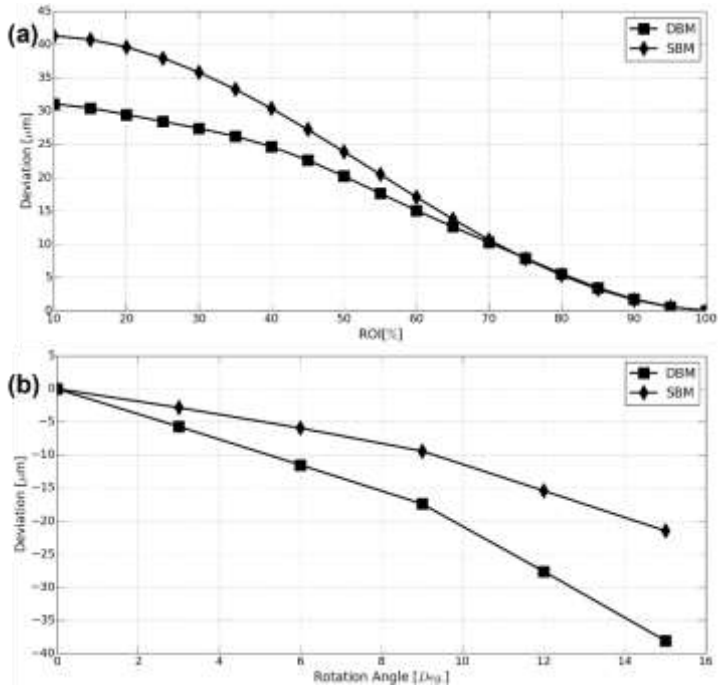

Both the 6 mm and 20 mm nominal rods are scanned along x and y directions at 3321 and 1377 different positions within the measurement region, respectively. The pixel calibration at the central position of the region is obtained for the 6 mm rod and used to determine the deviations from the nominal diameters for both rods. Figure 4 presents the colormaps of deviations obtained using both the DBM and SBM methods. Specifically, for the 6 mm rod, the DBM method yields an average absolute deviation of 0.38% with maximum deviation of 1.05% (Figure 4(a)), while the SBM method returns an average absolute deviation of 0.35% with a maximum deviation of 0.95% (Figure 4(b)). Calculations showed that the deviation values for a 6 mm rod were 62.97 um on average with the DBM method and 57.21 um with the SBM method. For the 20 mm rod, the DBM method generates a mean absolute deviation of 0.21% with a maximum value of 0.42% (Figure 4(c)), while the SBM method produces a mean absolute deviation of 0.17% with a maximum value of 0.40%. The average deviation values for a 20 mm rod using the DBM approach were 83.85 µm, while the SBM method yielded values of 79.99 µm. Based on the absolute deviations, the SBM method provides a higher accuracy of 0.25% of the nominal diameter, which is more precise than the DBM method with an accuracy of 0.46%.

Figure 4 Deviation in the Nominal Diameter of a 6 mm Rod (a)-(b) and a 20 mm Rod (c)-(d) Over Measurement Areas of 20 mm x 40 mm and 8 mm x 40 mm, Respectively, for the DBM (a)-(c) and SBM (b)-(d) Methods.

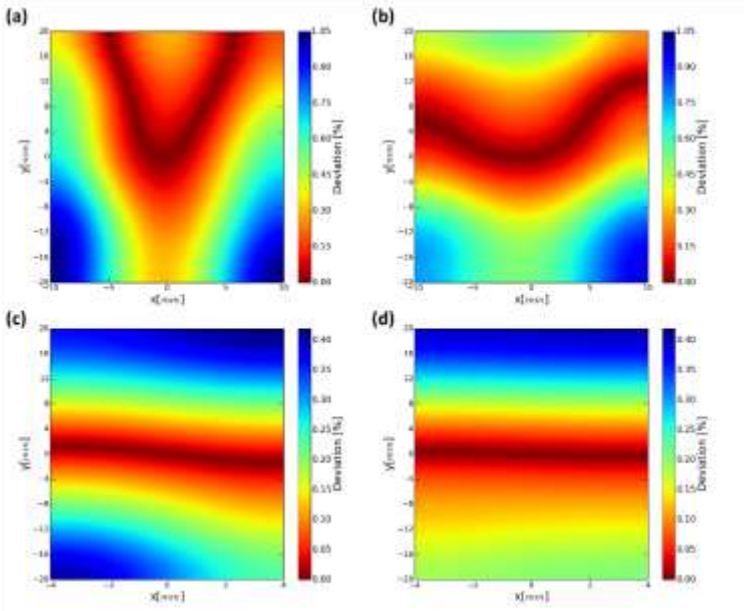

4. Discussion and Conclusion

Based on the literature review, the measured diameter range and standard deviation align with the prevailing findings in existing studies. Table 1 presents a comparative analysis between our investigation and relevant studies found in the literature. Notably, the utilization of telecentric lenses is highlighted in the comparison. To the best of our knowledge, among the referenced studies, none have undertaken dynamic measurements or aimed to integrate into dynamic systems. In our study, we conducted measurements of sample diameters without necessitating their fixed positioning. Our findings demonstrate that with a resolution of 10.93 µm, objects ranging from 4 to 27 mm in diameter can be measured with a standard deviation of 9.11 µm. Notably, our approach facilitates a wider range of motion for the objects under examination, without the need for fixation.

Table 1: Comparison of The Current Study with Other Related Studies.

Study	System	Telecentric Lens	Resolution (µm)	Diameter Range(mm)	Standard Deviation (µm)
[7]	Static	Yes	9.85	7-10	0.24
[12]	Static	Yes	-	6	10
[13]	Static	No	-	30-40	15
[14]	Static	No	-	8	12
Current Study	Dynamic	No	10.93	4-27	9.11

To summarize, this study presents a practical and low-cost optical system for measuring the diameters of continuous lines of round samples, specifically addressing the challenges of accurately measuring long fabricated specimens like rods that have non-linear movements. The proposed system achieves high

precision with a measurement accuracy of 0.25% of nominal diameter, and the integration of both hardware and software components results in a reliable solution suitable for a wide range of industrial and scientific applications. Offering potential benefits including reduced material waste, diminished scrap, and enhanced adherence to quality benchmarks, this system emerges as a compelling asset across various industries.

5. Acknowledgement

The authors would like to express their gratitude to Figen Dikilitaş for her invaluable assistance in providing insights into the processes employed in the cold drawing plant.

6. References

1. Groover MP. Fundamentals of Modern Manufacturing: Materials, Processes, and Systems. 2020.
2. Standard Specification for Steel Bar, Carbon and Alloy, Cold-Finished. American Society for Testing Materials n.d. https://doi.org/10.1520/A0108-18.
3. Szewczyk R, Zieliński C, Kaliczyńska M. Advances in Intelligent Systems and Computing 440 Challenges in Automation, Robotics and Measurement Techniques. n.d.
4. Mekid S, Ryu HS. Rapid vision-based dimensional precision inspection of mesoscale artefacts. Proc Inst Mech Eng B J Eng Manuf 2007;221:659–72. https://doi.org/10.1243/09544054JEM739.
5. Piotr Garbacz, Tomasz Giesko. Multi-camera Vision System for the Inspection of Metal Shafts n.d. https://doi.org/DOI 10.1007/978-3-319-29357-8_64.
6. Guo S, Zhang J, Jiang X, Yin P, Lei W. Mini milling cutter measurement based on machine vision. Procedia Eng, vol. 15, 2011, p. 1807–11. https://doi.org/10.1016/j.proeng.2011.08.336.
7. Dvoinishnikov S V., Rakhmanov V V., Kabardin IK, Meledin VG, Semenov DO. A Way of Edge Detection for Cylindrical Objects on an Image by the Shadow Method of Dimensional Control. Optoelectronics, Instrumentation and Data Processing 2022;58:30–5. https://doi.org/10.3103/S8756699022010034.
8. Li W, Wu J, Li D, Tian Y, Tian J. Telecentricity based measurement error compensation in the bilateral telecentric system. Measurement (Lond) 2019;147. https://doi.org/10.1016/j.measurement.2019.07.050.
9. Radil T, Fischer J, Kucera J. A Novel Optical Method of Dimension Measurement of Objects with Circular Cross-section, Institute of Electrical and Electronics Engineers (IEEE); 2007, p. 386–91. https://doi.org/10.1109/imtc.2006.328478.
10. Sun Q, Hou Y, Tan Q, Li C. Shaft diameter measurement using a digital image. Opt Lasers Eng 2014;55:183–8. https://doi.org/10.1016/j.optlaseng.2013.11.005.
11. Demeyere M, Rurimunzu D, Eugène C. Diameter measurement of spherical objects by laser triangulation in an ambulatory context. IEEE Trans Instrum Meas 2007;56:867–72. https://doi.org/10.1109/TIM.2007.894884.
12. Chen J, Hu C, Yu Z, Cui J, You X. Vision-based online detection system of support bar. 2016 IEEE International Conference on Information and Automation, IEEE ICIA 2016, Institute of Electrical and Electronics Engineers Inc.; 2017, p. 1594–9. https://doi.org/10.1109/ICInfA.2016.7832073.
13. Hao F, Shi JJ, Chen DL, Wang F, Hu YT. Shaft diameter measurement using digital image composition at two different object distances. IOP Conf Ser Mater Sci Eng, vol. 504, Institute of Physics Publishing; 2019. https://doi.org/10.1088/1757-899X/504/1/012097.

14. Rakhmanov V V., Dvoynishnikov S V., Semenov DO, Glavny VG. Cylinder diameter measurement with displacement and rotation error correction for non-telecentric optics. J Phys Conf Ser, vol. 1675, IOP Publishing Ltd; 2020. https://doi.org/10.1088/1742-6596/1675/1/012085.
15. Jensen K, Anastassiou D. Subpixel Edge Localization and the Interpolation of Still Images. IEEE Transactions on Image Processing 1995;4:285–95. https://doi.org/10.1109/83.366477.
16. Wang X. Interpolation and Sharpening for Image Upsampling, Institute of Electrical and Electronics Engineers (IEEE); 2022, p. 73–7. https://doi.org/10.1109/iccgiv57403.2022.00020.
17. Siu W-C, Hung K-W. Review of Image Interpolation and Super-resolution. 2012.
18. Rostykus M, Rossi M, Moser C. Compact lensless subpixel resolution large field of view microscope. Opt Lett 2018;43:1654. https://doi.org/10.1364/ol.43.001654.
19. Flesia AG, Ames G, Bergues G, Canali L, Schurrer C. Sub-pixel straight lines detection for measuring through machine vision. Conference Record - IEEE Instrumentation and Measurement Technology Conference, Institute of Electrical and Electronics Engineers Inc.; 2014, p. 402–6. https://doi.org/10.1109/I2MTC.2014.6860776.
20. HajiRassouliha A, Taberner AJ, Nash MP, Nielsen PMF. Subpixel phase-based image registration using Savitzky–Golay differentiators in gradient-correlation. Computer Vision and Image Understanding 2018;170:28–39. https://doi.org/10.1016/j.cviu.2017.11.003.
21. Wang L, Zhang Y, Feng J. On the Euclidean distance of images. IEEE Trans Pattern Anal Mach Intell 2005;27:1334–9. https://doi.org/10.1109/TPAMI.2005.165.
22. Wang Z, Feng J, Yan S, Xi H. Linear distance coding for image classification. IEEE Transactions on Image Processing 2013;22:537–48. https://doi.org/10.1109/TIP.2012.2218826.